

Remote sensing of radioactive alteration zones using Sentinel-2 and SPAD chlorophyll measurements in Mamuju, Indonesia

Rudarsko-geološko-naftni zbornik
(The Mining-Geology-Petroleum Engineering Bulletin)
DOI: 10.17794/rgn.2026.3.14

Original scientific paper



Nuraisyiah Pertiwi Kamsir¹ , Asep Saepuloh^{1*} , Very Susanto¹ , Eka Djatnika Nugraha² 

¹ Geological Engineering, Faculty of Earth Sciences and Technology, Institut Teknologi Bandung, Jl. Ganesha No. 10 Bandung, Indonesia.

² Research Center for Safety, Metrology, and Nuclear Quality Technology, Research Organization of Nuclear Technology, The National Research and Innovation Agency of Indonesia (BRIN), Tangerang Selatan 15314, Banten, Indonesia.

Abstract

This study investigates natural radioactive mineralization (uranium–thorium) in Mamuju, West Sulawesi, particularly within the fault-controlled Adang Volcanics, an area known for anomalous natural radiation. The objective was to evaluate vegetation stress as a proxy for radioactive mineralization by integrating satellite data and field validation. We processed Sentinel-2A data using band ratios (4/2 iron oxide, 4/3 ferric iron, 11/12 clay) and false colour composites to delineate alteration zones. The Red Edge Vegetation Index (REVI; B3, B4, B6) was calculated to detect vegetation stress. Fieldwork in December 2023 collected 68 SPAD chlorophyll measurements from ferns, interpolated with inverse distance weighting, and compared with independent radiation dose rates. The results show a strong correlation between REVI and SPAD ($R^2 = 0.76$), confirming the sensitivity of red-edge bands to chlorophyll variability. SPAD values decreased significantly in high-radiation zones, showing a strong negative correlation with dose rate ($R^2 = 0.90$). Values of 4–40 were typical in anomalous radiation areas, while >40 characterized lower exposure. Vegetation stress anomalies and satellite-derived Chlorophyll Index overlapped spatially with alteration zones and were concentrated in the Adang Volcanics along structural controls. Species differences among ferns indicated varied sensitivity to radiation. This integrated approach demonstrates the effectiveness of Sentinel-2 alteration composites, REVI, and SPAD validation as a rapid, low-cost framework for early exploration of radioactive minerals while also contributing to environmental radiation hazard assessment.

Keywords:

Sentinel-2, Red Edge Vegetation Index (REVI), SPAD chlorophyll, radioactive mineralization, Mamuju

1. Introduction

Indonesia has long been recognized as a country with considerable potential for uranium and thorium resources, which are strategically distributed across several major islands, including Sumatra, Kalimantan, and Sulawesi (Aditya et al., 2025; Saputra et al., 2025). Among these regions, Mamuju in West Sulawesi stands out as an area with naturally high radiation dose rates compared to its surroundings (Nugraha et al., 2021). This anomaly is closely linked to the geological setting, where volcanic rock formations host uranium- and thorium-bearing minerals (Saepuloh et al., 2023). These minerals may occur as primary deposits formed via magmatic and hydrothermal processes, or as secondary accumulations derived from sedimentary processes and intense weathering (Subasinghe et al., 2022). The natural enrichment of these radioactive elements makes Mamuju an area of

dual significance (Nugraha et al., 2021). On the one hand, it represents a potential energy resource that could support future nuclear power development as part of a sustainable energy transition. On the other hand, the elevated levels of radiation exposure in the environment pose a serious concern, particularly for local ecosystems and human health (Bréchnignac et al., 2016). Long-term exposure to ionizing radiation is known to increase risks of cancer, genetic disorders, and other health problems, which underlines the importance of comprehensive studies to better understand the geological and environmental dynamics of this area.

Exploration of radioactive mineralization in such complex environments requires innovative methods that are both effective and practical. Conventional ground-based surveys, although accurate, are often costly, time-consuming, and difficult to implement in regions with rugged terrain or dense vegetation (Abdulraheem et al., 2023). Remote sensing has emerged as an alternative approach that can provide broad spatial coverage and detailed information without the need for direct physical access to every location (Yu & Fang, 2023). By record-

* Corresponding author: Asep Saepuloh

e-mail address: saepuloh@itb.ac.id

Received: 4 September 2025. Accepted: 28 December 2025.

Available online: 14 May 2026

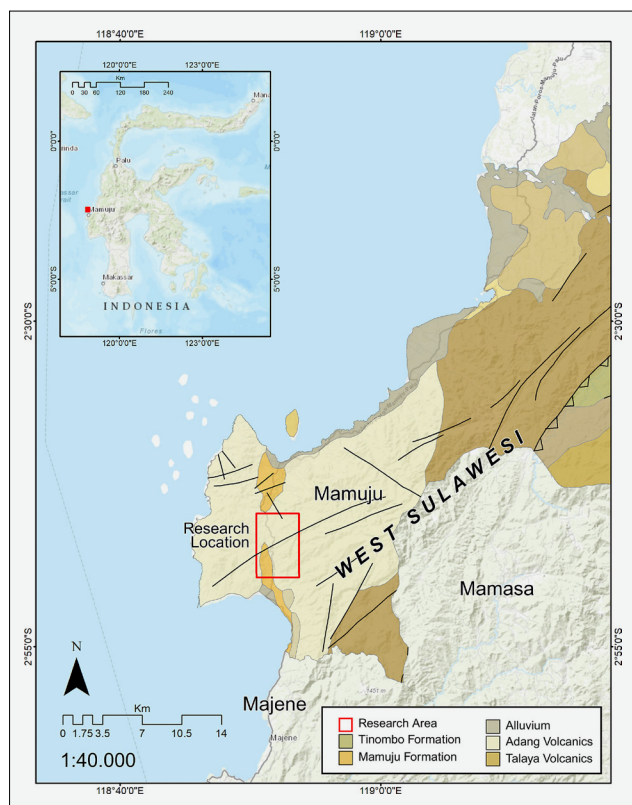


Figure 1. Geological formations in the Mamuju study area showing the distribution of the Mamuju Formation and Adang Volcanics, the only formations present within the study area, along with major faults controlling the structural framework.

ing and analyzing the spectral response of the Earth's surface to solar radiation, satellite sensors are capable of differentiating materials based on their reflectance characteristics. Sentinel-2, for instance, offers high-resolution multispectral data that can highlight zones of mineral alteration and other surface anomalies. However, the interpretation of satellite imagery is not without challenges (Chen et al., 2023; Hu et al., 2018). Disturbances from atmospheric particles, cloud cover, and particularly dense vegetation can significantly reduce the clarity of spectral signals, thereby complicating the detection of underlying lithological features (Meraner et al., 2020; Shebl et al., 2024). These limitations highlight the necessity of developing techniques that are able to extract meaningful information even under conditions where direct mineral signals are obscured.

Previous studies (Rosiana et al., 2020; Saepuloh et al., 2023) have shown that vegetation cover poses a major challenge for mineral exploration using optical satellite imagery, particularly in tropical regions like Mamuju, where a dense canopy often obscures the spectral characteristics of rocks and minerals and reduces the effectiveness of conventional remote sensing methods. A geobotanical approach offers a way to overcome this limitation by leveraging the principle that plants reflect the geochemical conditions of their substrate, as vegeta-

tion can absorb metals and radionuclides from the soil, affecting physiological processes such as chlorophyll activity, water uptake, and photosynthesis. Although these stress responses are not always visually apparent, they can be detected through changes in leaf spectral reflectance, particularly in the visible and red-edge regions of the electromagnetic spectrum, making plants potential natural bioindicators of subsurface mineralization.

While the use of vegetation stress as a mineral exploration tool is widely recognized, its application in areas with naturally occurring radioactive minerals in Indonesia remains limited, highlighting opportunities for research that integrates geological, biological, and remote sensing perspectives. By combining remote sensing techniques with vegetation-based indicators, this approach provides an alternative means to investigate regions where direct lithological observation is constrained by forest cover, interpreting vegetation stress as a potential signal of underlying geological conditions associated with radioactive mineralization. The findings are expected to advance both the scientific understanding of geobotanical responses in radioactive environments and practical considerations for natural resource assessment and environmental risk evaluation.

2. Geological Setting

The study area is located in Mamuju, West Sulawesi, within a complex tectonic setting at the junction of the Australian Plate, Sunda Plate, and Philippine Sea Plate, which has produced active faulting and structural deformation (Somptan, 2012; Supendi et al., 2021). The geology of the region is dominated by volcanic and sedimentary formations (Laode et al., 2025), with the Mamuju Formation and Adang Volcanics as the primary units in the study area, as shown in Figure 1. The Mamuju Formation consists of marl, calcareous sandstone, coral limestone, and tuffaceous sandstone, occasionally interbedded with conglomerate and claystone, reflecting a shallow marine depositional environment characterized by weakly lithified carbonate and volcanoclastic sediments (Perdana & Amijaya, 2011; White et al., 2017). The Adang Volcanics comprises volcanic rocks with phonolitic leucite composition containing minerals such as leucite, K-feldspar, plagioclase, pyroxene, and minor opaque minerals, which are generally moderately to strongly weathered (Shaban et al., 2016).

Faults are present throughout the study area, controlling the structural framework and influencing the distribution and deformation of both sedimentary and volcanic units (Meilano et al., 2023; Supendi et al., 2021). These faults contribute to variations in topography and rock stability, shaping the landscape of Mamuju and affecting the lithological expression of the Mamuju Formation and Adang Volcanics. The combination of volcanic and sedimentary rocks with active fault structures provides a

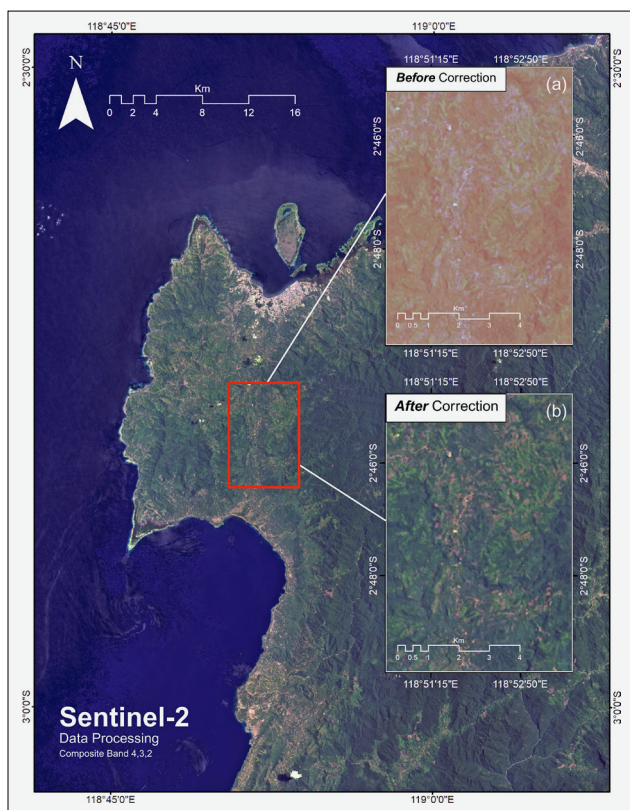


Figure 2. Sentinel-2 imagery before (a) and after (b) correction, showing the improvement in visual quality and spatial alignment.

unique geological setting for examining mineralization patterns, geohazard potential, and the interaction between tectonics and rock properties in the region.

3. Data and Satellite Image Processing

3.1. Data

The primary dataset used in this research is Sentinel-2A multispectral imagery acquired on **October 9, 2019** with less than 10% cloud cover. Sentinel-2 provides 13 spectral bands in the visible, red-edge, near-infrared, and shortwave infrared regions with spatial resolutions ranging from 10 to 60 meters (Bayle et al., 2019; Liu et al., 2021). For this study, nine bands were utilized due to their spectral relevance for both mineralogical and veg-

etation analysis. Details of the spectral bands used are summarized in **Table 1**.

Complementary data included a **geological map of the Mamuju sheet** from Geomap (Indonesian Geological Agency), and a **radiation dose-rate dataset** compiled by Wijaya (2024). These were employed to provide lithological context and independent validation of remote sensing results. The field survey conducted in December 2023 yielded **68 SPAD chlorophyll measurements** on ferns, which served as ground-truth data for vegetation stress evaluation. Each measurement was taken at three points of a leaf (tip, middle, and base) to reduce intra-sample variability.

3.2. Satellite Imagery Data Processing

The Sentinel-2 image was pre-processed through atmospheric and radiometric corrections to convert raw digital numbers into surface reflectance values (Rumora et al., 2021; Vrdoljak & Kilić Pamuković, 2022). Geometric correction was conducted to align the image to UTM Zone 50S, WGS84 datum, as shown in **Figure 2**. A pan-sharpening enhancement was also applied to improve the spatial detail of multispectral bands. For mineralogical analysis, band ratio techniques were applied to exploit the spectral differences between absorption and reflectance features of alteration minerals. The following ratios were selected (Carvalho et al., 2025; Saepuloh et al., 2023):

- Band 4 / Band 2 → iron oxide (hematite, goethite)
- Band 4 / Band 3 → ferric iron minerals
- Band 11 / Band 12 → clay minerals (illite, kaolinite, smectite)

These ratio layers were subsequently combined into a false-colour composite (R: 4/3, G: 4/2, B: 11/12), allowing the discrimination of alteration zones that are frequently associated with uranium and thorium enrichment. The results of the band ratio composites are presented in **Figure 3**.

3.2.1. Red Edge Vegetation Index (REVI)

Vegetation stress was analyzed using the Red Edge Vegetation Index (REVI), which is particularly sensitive to changes in chlorophyll content and has proven effective in detecting vegetation stress under environmental

Table 1. Summary of the dataset and band features of the Sentinel-2 images employed in this study

Date of acquisition	Band Name	Wavelength range (µm)	Resolution (m)
October 9, 2019	B2 Visible (blue/B)	0.458–0.523	10
	B3 Visible (green/G)	0.543–0.578	10
	B4 Visible (red/R)	0.650–0.680	10
	B5 Red edge-1 (RE-1)	0.698–0.713	20
	B11 Shortwave infrared-1 (SWIR-1)	1.565–1.655	20
	B12 Shortwave infrared-2 (SWIR-2)	2.100–2.280	20

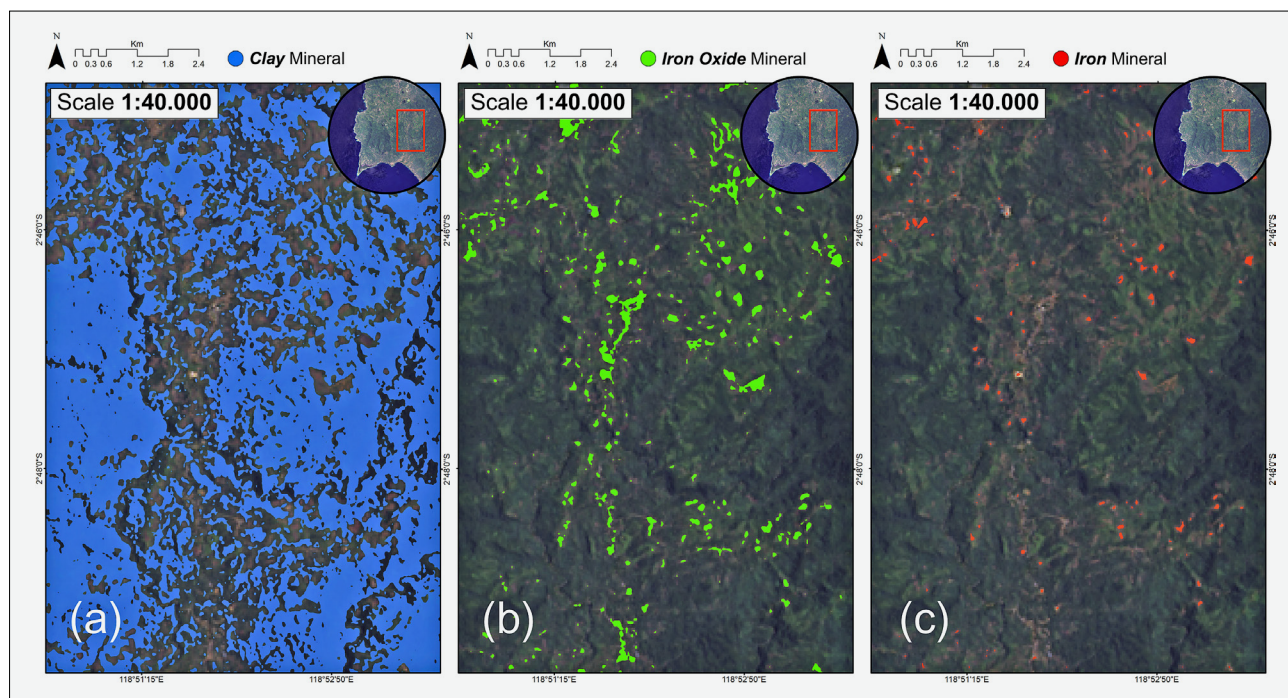


Figure 3. Band ratio composites for hydrothermal alteration mapping: (a) clay minerals (illite, kaolinite, smectite) highlighted using Band 11/Band 12 (blue), (b) iron oxide minerals (hematite, goethite) mapped using Band 4/Band 2 (green), and (c) ferric iron minerals extracted from Band 4/Band 3 (red).

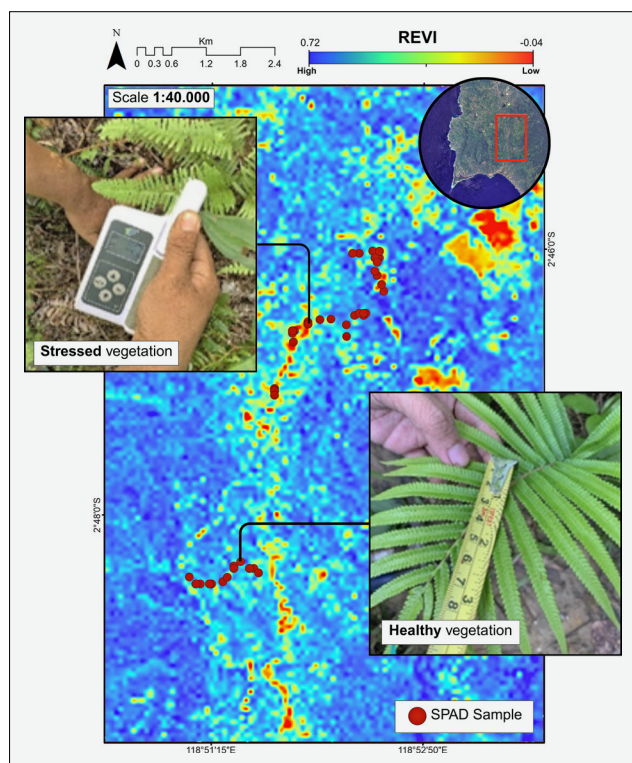


Figure 4. Spatial distribution of the Red Edge Vegetation Index (REVI), where the colour gradient from red to blue reflects variations in vegetation density, with higher values (blue) indicating denser and healthier vegetation cover. The brown dots represent SPAD sampling locations used for ground-truth validation.



Figure 5. Field documentation of SPAD verification: (a) SPAD measurement on ferns exhibiting stunted growth and pale green colouration; and (b) SPAD measurement on ferns with healthy appearance and greener leaves.

anomalies such as radioactive exposure (Dong et al., 2019; Sun et al., 2020). The index was calculated as (Saepuloh et al., 2023):

$$REVI = \frac{B3 - B4}{B3 + B4} + \frac{B6 - B4}{B6 + B4} \quad (1)$$

Where:

- B3 – the green band (0.543–0.578 μm),
- B4 – the red band (0.650–0.680 μm),
- B6 – the red-edge band (0.733–0.748 μm).

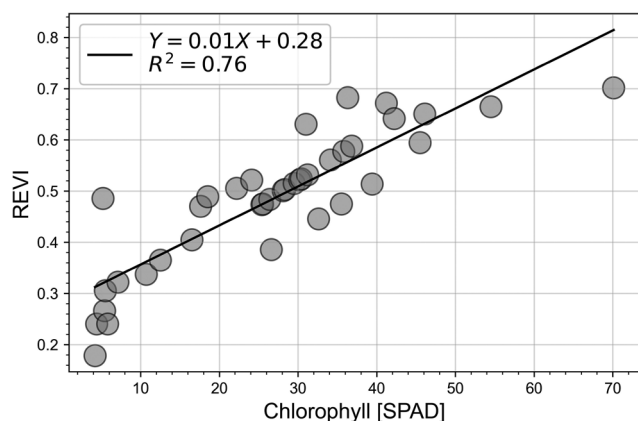


Figure 6. Correlation between field-measured SPAD values and the Red Edge Vegetation Index (REVI), showing a strong positive relationship with $R^2 = 0.76$, indicating that satellite-based vegetation indices effectively capture chlorophyll variation observed in the field.

The REVI map clearly highlights spatial variations in vegetation health, with lower values indicating stressed vegetation. This index was selected as the primary remote sensing proxy for bioindicator analysis in relation to radioactive mineralization. The results of the REVI analysis are shown in **Figure 4**.

3.3. Field Chlorophyll Measurement

Field surveys were conducted in December 2023 to obtain in-situ validation data. A total of 68 ferns were sampled across Botteng and Salumatti villages. Chlorophyll content was measured using a SPAD chlorophyll meter, which estimates relative chlorophyll concentration by analyzing light transmission in red and near-infrared wavelengths. The collected SPAD values were interpolated spatially using the Inverse Distance Weighting (IDW) method in ArcGIS to generate continuous chlorophyll distribution maps. Morphological observations, such as leaf discoloration and growth inhibition, were recorded to complement quantitative SPAD data, with the sampling locations shown in **Figure 4** and field documentation presented in **Figure 5**.

3.4. Data Integration and Validation

Data integration was performed to link remote sensing results with ground measurements and radiation data. First, alteration mineral composites from band ratios were overlaid with interpolated SPAD maps to examine spatial correspondence between alteration zones and vegetation stress. Second, correlation analysis was conducted between measured SPAD values and radiation dose rates, as well as between SPAD and REVI. As shown in **Figure 6**, REVI exhibited a strong positive correlation with SPAD ($R^2 = 0.76$), indicating that satellite-based vegetation indices reliably reflect field-measured chlorophyll content. Regression modelling was then applied to derive satellite-based chlorophyll esti-

mates (Chlorophyll Index), enabling the extrapolation of field observations across the study area. This integrative approach ensured that anomalies identified in the satellite imagery corresponded with field-verified vegetation stress and geological context, thereby increasing the reliability of remote sensing for preliminary radioactive mineral exploration.

4. Results and Discussion

4.1. SPAD Measurements and Radiation Dose Rates

Field-based chlorophyll measurements revealed a pronounced physiological response of ferns to elevated natural radiation. Across 68 samples, SPAD values ranged from 4 to 40, with the lowest values consistently recorded in zones of higher radiation dose rates. However, only 38 of these samples had spatially corresponding radiation measurements from the Wijaya (2024) dataset within an acceptable matching distance, and thus this subset ($n = 38$) was used for correlation and ANOVA analyses to ensure spatial comparability. Conversely, areas characterized by lower radiation levels exhibited markedly higher and more stable SPAD values (>40) (see **Figure 7**). When compared against radiation dose rates reported by **Wijaya (2024)**, the dataset demonstrated a strong negative correlation ($R^2 = 0.90$), providing robust evidence that increasing radiation levels directly suppress chlorophyll content in vegetation (see **Figure 8**).

To further evaluate whether chlorophyll levels differ systematically across radiation environments, radiation dose rates were grouped into three classes based on the empirical distribution of the dataset: low (< 3206 nSv/h), moderate (3206–4925 nSv/h), and high (> 4925 nSv/h). The summary statistics for these radiation classes are presented in **Table 2**, which clearly shows a monotonic decline in SPAD values with increasing radiation intensity. Mean SPAD decreases from 42.3 ± 10.3 in the low-radiation class to 28.1 ± 2.4 in the moderate class and sharply declines to 10.4 ± 6.3 in the high-radiation class, indicating progressively stronger physiological suppression under elevated radiation conditions.

A one-way ANOVA was conducted to determine whether these observed differences in SPAD among radiation classes were statistically significant. The ANOVA results, summarised in **Table 3**, demonstrate a highly significant effect of radiation class on chlorophyll content ($F(2,35) = 63.84$, $p < 0.0001$). The effect size ($\eta^2 = 0.78$) indicates that approximately 78% of the variance in SPAD is attributable to differences in radiation level, underscoring the dominant role of natural radioactivity in shaping vegetation physiological response. Post-hoc Tukey HSD tests confirmed that all three radiation classes differ significantly from one another ($p \leq 0.001$), meaning that SPAD in the high-radiation class is significantly lower than in both the moderate- and low-radia-

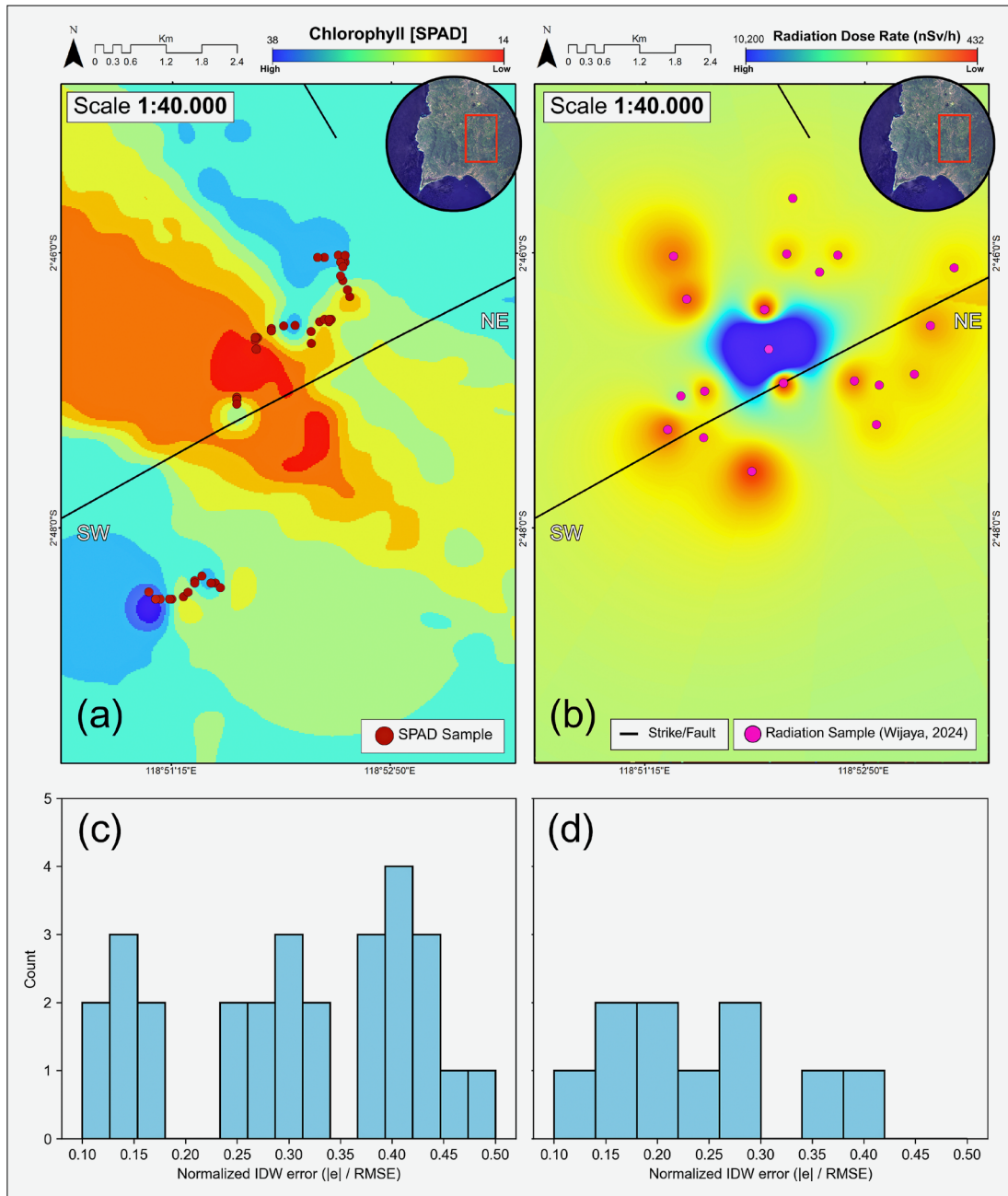


Figure 7. Spatial distribution maps showing (a) interpolated SPAD Chlorophyll Index from 68 fern samples, and (b) natural radiation dose rates adapted from Wijaya (2024). Lower SPAD values (4–40) are associated with zones of higher radiation, while higher values (>40) occur in areas with lower radiation exposure. (c) presents the normalized IDW interpolation error for the SPAD dataset, illustrating the distribution of uncertainty associated with the chlorophyll interpolation surface. (d) The corresponding normalized IDW interpolation error for the radiation exposure rate dataset, providing an assessment of spatial reliability for the radiometric interpolation.

tion classes, and that the moderate class also differs significantly from the low-radiation class.

Assumption checks indicated no significant heterogeneity of variances (Levene’s test, $p = 0.11$), while minor deviations from normality were detected in residuals. Given the balanced group sizes, the strong separation of class means, and the large effect size, the ANOVA results are considered robust. Collectively, the regression results and the class-level analysis presented in **Table 2**

and **Table 3** provide compelling statistical evidence that elevated natural radiation consistently suppresses chlorophyll content and contributes to measurable physiological stress in vegetation across the study area.

4.2. Chlorophyll Index Distribution and Alteration Mineral Composites

The spatial distribution of Chlorophyll Index was systematically compared with alteration anomalies derived

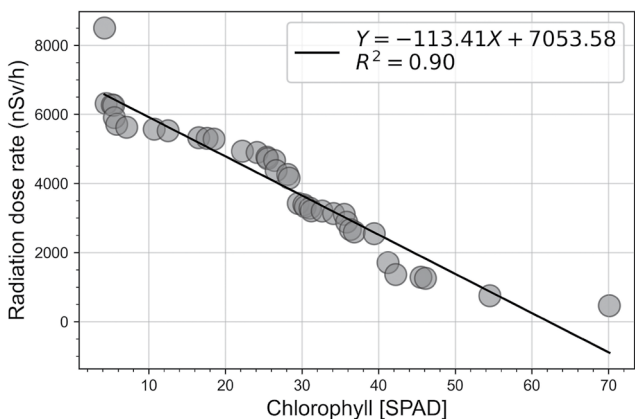


Figure 8. Relationship between SPAD Chlorophyll Index and natural radiation dose rates (Wijaya, 2024), showing a strong negative correlation ($R^2 = 0.90$) that indicates increasing radiation levels directly reduce chlorophyll content in vegetation.

Table 2. Descriptive statistics of SPAD Chlorophyll Index across radiation classes

Radiation Class	Dose-rate Range (nSv/h)	n	Mean SPAD	SD
Low	< 3206	13	42.32	10.30
Moderate	3206–4925	12	28.06	2.43
High	> 4925	13	10.43	6.33

Table 3. One-way ANOVA results for SPAD across radiation classes

Source	SS	df	MS	F	p-value
Between groups	6631.41	2	3315.70	63.84	< 0.0001
Within groups	1817.87	35	51.94	–	–
Total	8449.28	37	–	–	–

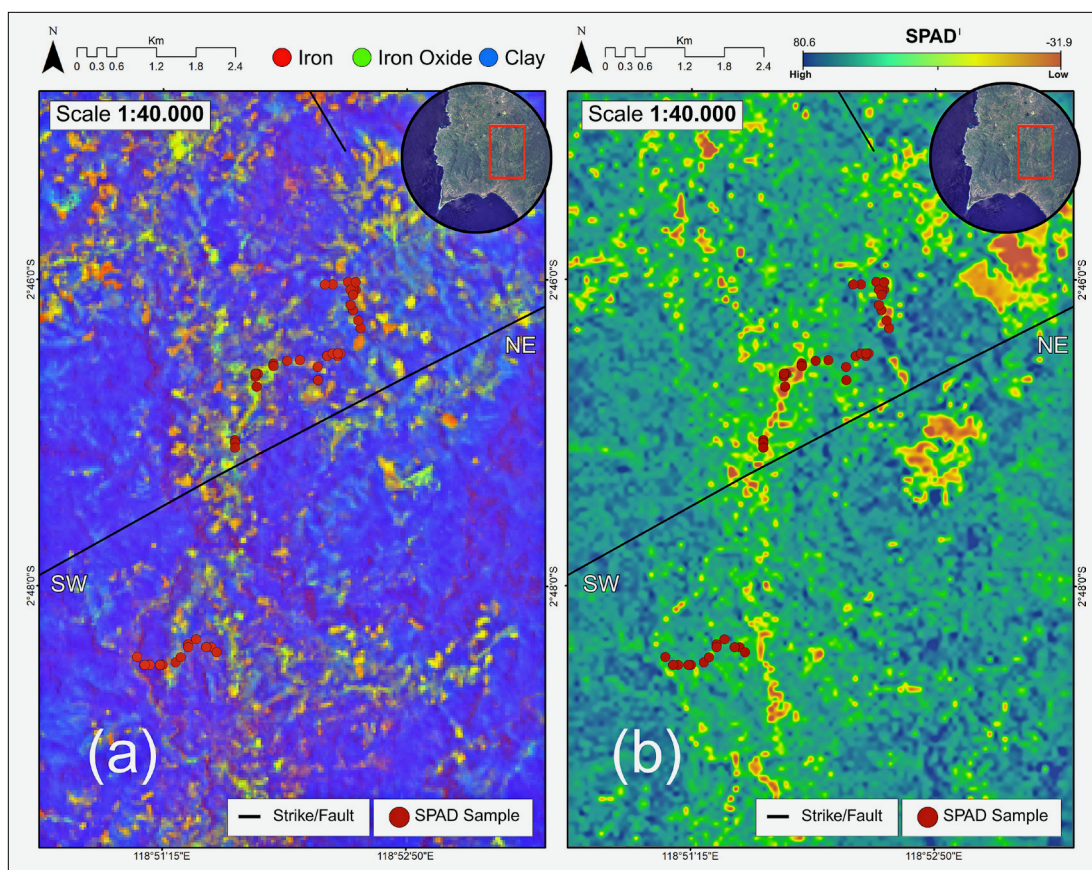


Figure 9. Comparison between vegetation and mineral alteration anomalies. (a) Mineral band ratio composite ($R = 4/3, G = 4/2, B = 11/12$). (b) spatial distribution of Chlorophyll Index values indicating chlorophyll content, and the black lines indicate mapped faults.

from Sentinel-2 band ratio composites. The false-colour composite ($R = 4/3, G = 4/2, B = 11/12$) proved effective in delineating three key alteration indicators, namely iron oxides (Band Ratio 4/2), ferric iron minerals (Band Ratio 4/3), and clay minerals (Band Ratio 11/12). These alteration signatures are not randomly distributed but are prominently concentrated in the volcanic rocks of the

Adang Formation, which have long been recognized as zones of hydrothermal activity. As shown in **Figure 9**, the composite map reveals that areas characterized by strong alteration signatures correspond closely with zones of reduced Chlorophyll Index values, thereby suggesting a spatial link between mineralogical alteration and vegetation stress.

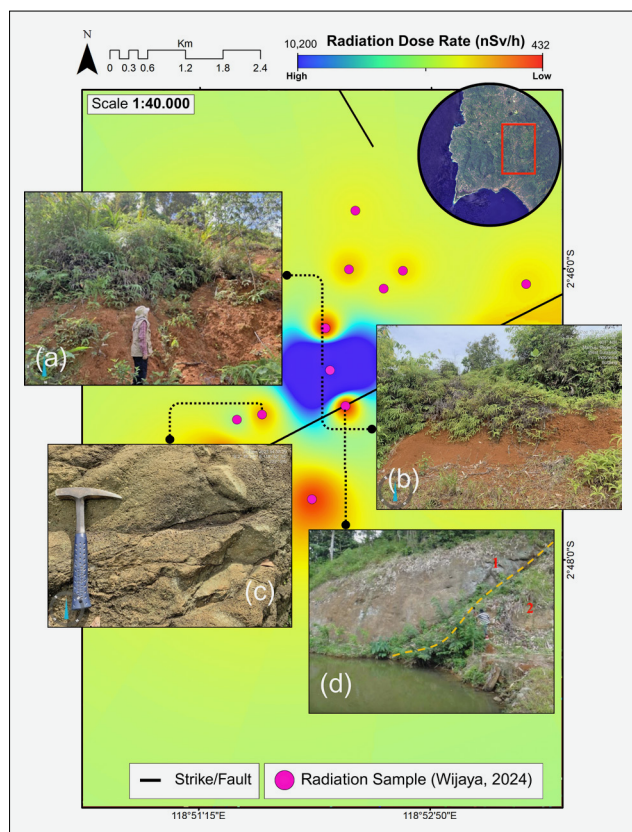


Figure 10. Field verification within the Adang volcanic terrain revealed (a) outcrops showing pervasive hydrothermal alteration of volcanic rocks, (b) vegetation growing on weathered products of altered rocks that exhibited clear stress responses, including low SPAD values and reduced leaf size, (c) basaltic lithology characterized by phenocrysts dominated by leucite minerals, and (d) a distinct lithological contact between phonolitic lava (unit 1) and volcanic breccia (Rahmaningrum, 2025).

Ground-based verification provided further confidence in this interpretation (see **Figure 10**). Field surveys conducted within the Adang volcanic terrain revealed rocks that have undergone pervasive hydrothermal alteration. These rocks exhibited clear mineralogical transformations, such as clay replacement and extensive iron oxide staining, which are consistent with processes of alteration linked to fluid–rock interactions in a volcanic setting. Vegetation growing on soils derived from these altered substrates showed distinct stress responses, including markedly low Chlorophyll Index values (commonly below 30), reduced leaf size, and visible discoloration ranging from chlorosis to reddish pigmentation. These symptoms reflect impaired chlorophyll content and overall physiological stress, and they align well with the remote sensing observations of vegetation decline in areas of strong alteration anomalies.

This convergence of remote sensing analysis and field verification underscores the diagnostic strength of integrating Chlorophyll Index measurements with mineral alteration composites. The reduced chlorophyll content observed in vegetation is not merely coincidental but ap-

pears to be directly linked to the geochemical environment of radionuclide-bearing alteration zones. The association highlights how vegetation stress indicators can act as a proxy for detecting subsurface mineralogical processes.

In interpreting the REVI patterns, it is important to note that red-edge reflectance is still influenced by several external factors, including thin cloud cover, haze, terrain-induced shadows, and seasonal phenology, all of which may affect the accuracy of chlorophyll estimation. Since this analysis relies on a single-date Sentinel-2 acquisition, part of the observed variability could reflect seasonal changes in pigment concentration or canopy condition rather than purely radiation-driven stress. To address this limitation, NDVI was computed as a complementary vegetation index. Although less sensitive to chlorophyll variation than REVI, NDVI exhibited spatial trends that were consistent with REVI, particularly in high-radiation areas, as shown in **Figure 11**. This agreement strengthens the interpretation that the detected spectral anomalies represent genuine vegetation stress rather than artefacts of illumination or seasonal effects, thereby directly addressing the reviewer’s request for clarification of REVI limitations and the inclusion of an alternative index for validation.

4.3. Integrated Overlay of Chlorophyll Index, Radiation, and Geological Framework

The final stage of analysis involved integrating Chlorophyll Index, radiation dose-rate data, and the geological framework to examine spatial controls. The radiation dataset used in this study was derived from **Wijaya (2024)**, who mapped the spatial distribution of natural radiation in the research area. The overlay between Chlorophyll Index distribution and radiation dose-rate maps clearly demonstrates a consistent negative correlation: areas characterized by elevated radiation exposure display markedly low Chlorophyll Index values, whereas zones with lower radiation are associated with higher chlorophyll content. This spatial pattern underscores the direct influence of surface radioactivity on vegetation physiology, particularly its role in reducing chlorophyll concentration. The regions of strong radiation anomalies overlap with vegetation exhibiting stress responses, thereby reinforcing the reliability of Chlorophyll Index as a sensitive biophysical indicator of radiation exposure. These findings are in agreement with the results reported by **Wijaya (2024)**, who observed significant chlorophyll reduction in high-radiation zones. The consistency between this study and previous research strengthens the validity of employing Chlorophyll Index as a physiological proxy for detecting radiation stress in vegetation. Importantly, the correlation highlights the potential of plant-based measurements to serve as an indirect yet effective method for mapping radiation hazards in the field, offering a complementary approach to conventional radiometric surveys.

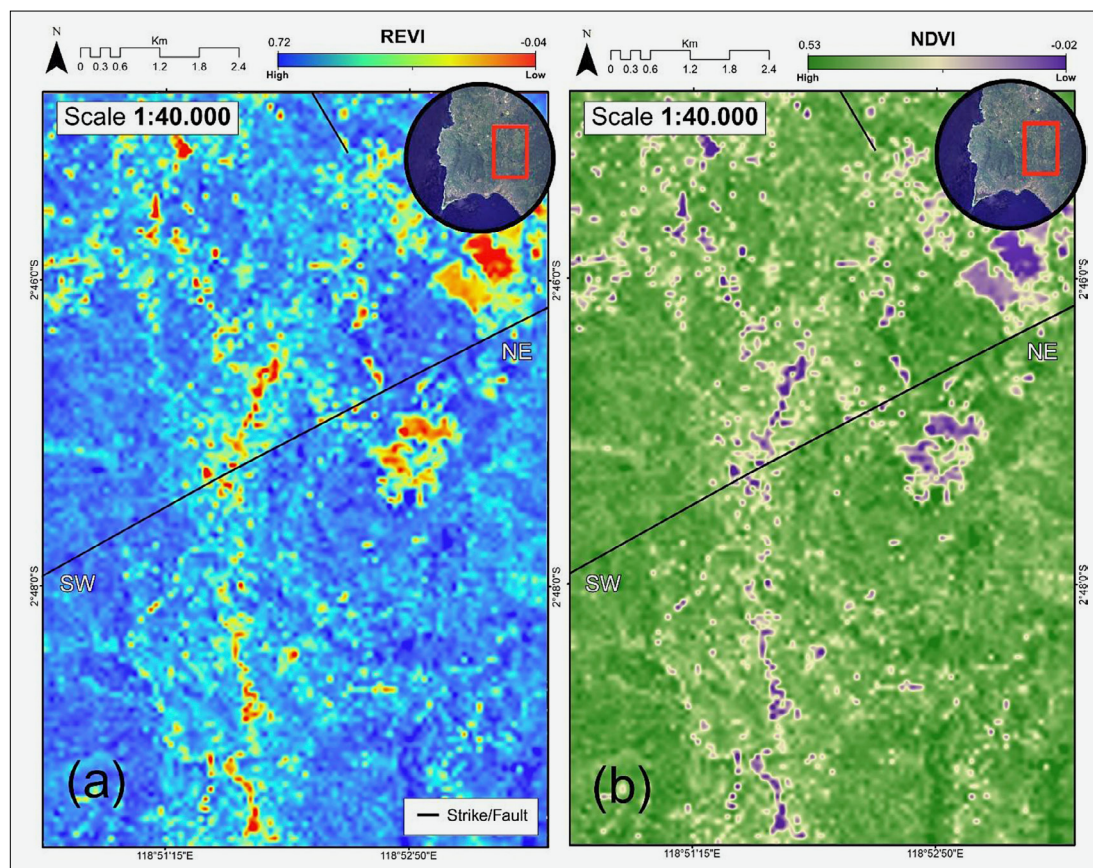


Figure 11. (a) REVI map highlighting vegetation stress zones associated with elevated natural radiation, showing pronounced reductions in red-edge reflectance across the Adang Volcanics. (b) NDVI map derived from the same Sentinel-2 acquisition, which although less sensitive to chlorophyll variation, exhibits spatial patterns consistent with the REVI distribution, particularly in high-radiation areas.

The relationship between Chlorophyll Index and radiation is not only spatially coherent but also strongly linked to the geological setting (see **Figure 12**). Lithological and structural factors exert primary control over the occurrence and intensity of radioactive anomalies. High-radiation zones are predominantly associated with lava flows of Botteng and the Tapalang breccia, both of which belong to the Adang Volcanic Formation. These rocks are dominated by phonolite and leucite-bearing basalt, lithologies with ultrapotassic affinities that are geochemically favorable for the presence of uranium- and thorium-bearing minerals. Consequently, the distribution of Chlorophyll Index values mirrors the underlying lithological variation, with vegetation stress responses most evident on soils derived from radiation-rich volcanic units.

In addition to lithology, structural geology also plays a critical role. Fault zones and remnant topographic highs of the Adang volcanic edifice are interpreted as pathways for hydrothermal fluid mobilization. These fluids likely transported radioactive elements such as uranium and thorium, leading to localized mineral precipitation and the formation of high-radiation zones. Vegetation responses captured through Chlorophyll Index measurements follow this structural control, further

supporting the hypothesis that both lithology and tectonic structures dictate the spatial variability of radiation and its ecological impacts.

5. Conclusions

This study demonstrates that the integration of remote sensing and a geobotanical approach provides an effective framework for detecting radioactive mineralization in vegetation-covered regions such as Mamuju, West Sulawesi. By linking Sentinel-2 band ratio composites, red-edge vegetation indices, and in-situ chlorophyll measurements, vegetation stress was shown to reliably reflect the distribution of uranium–thorium–bearing lithologies and hydrothermal alteration zones. The strong spatial correspondence between reduced chlorophyll content, elevated radiation levels, and volcanic units of the Adang Formation underscores the potential of vegetation bioindicators as indirect proxies for subsurface mineralization and environmental radiation hazards.

Despite these promising results, several limitations remain. Environmental factors such as soil moisture, pH, nutrient availability, and micro-topographic shading could not be incorporated due to the lack of spatially matched measurements and may contribute to residual

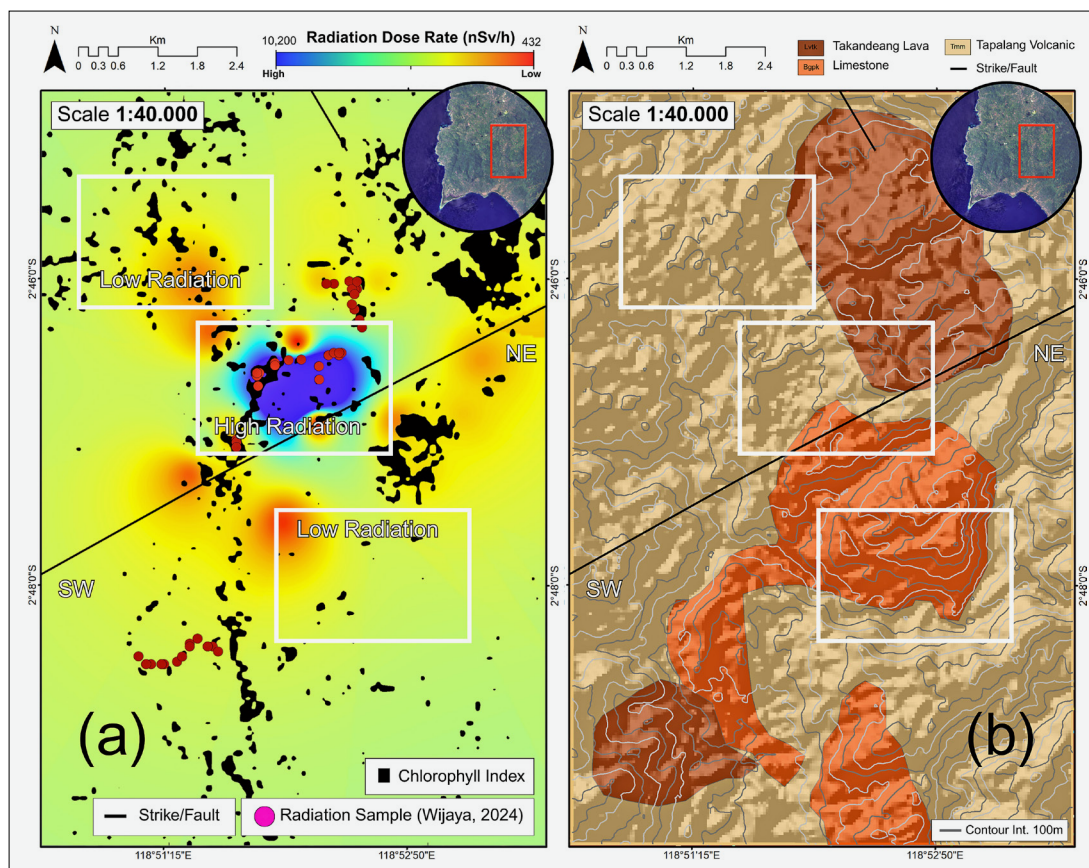


Figure 12. Relationship between vegetation stress and geological controls: (a) overlay of Chlorophyll Index distribution with natural radiation dose rates adapted from **Wijaya (2024)**, showing inverse correlation between radiation intensity and chlorophyll content, and (b) contour and lithological map of the study area illustrating that high-radiation anomalies are primarily concentrated within volcanic units of the Adang Formation

variability in the chlorophyll indicators. In addition, variability in species-specific responses to radiation, seasonal influences on vegetation physiology, and the moderate spatial resolution of Sentinel-2 imagery may constrain the broader applicability of the method. Future research should combine higher-resolution satellite data, expanded species monitoring, and geochemical sampling to improve accuracy and strengthen the interpretative framework. These findings mark an important step toward developing cost-effective exploration and monitoring strategies that address both natural resource potential and environmental health concerns in high-radiation landscapes.

Acknowledgement

This research is funded by the Indonesian Endowment Fund for Education (LPDP) on behalf of the Indonesian Ministry of Higher Education, Science and Technology and managed under the EQUITY Program (Contract No. 4298/B3/DT.03.08/2025), as well as the PPMI FITB Program from the Faculty of Earth Sciences and Technology ITB Research Scheme Number (Contract No. 2235/IT1.B07.1/TA.00/2026).

6. References

- Abdulraheem, M. I., Zhang, W., Li, S., Moshayedi, A. J., Farooque, A. A., & Hu, J. (2023). Advancement of Remote Sensing for Soil Measurements and Applications: A Comprehensive Review. *Sustainability (Switzerland)*, *15*(21). <https://doi.org/10.3390/su152115444>
- Aditya, I. A., Wijayanto, T., & Hakam, D. F. (2025). Advancing Renewable Energy in Indonesia: A Comprehensive Analysis of Challenges, Opportunities, and Strategic Solutions. *Sustainability (Switzerland)*, *17*(5), 2021–2030. <https://doi.org/10.3390/su17052216>
- Bayle, A., Carlson, B. Z., Thierion, V., Isenmann, M., & Choler, P. (2019). Improved mapping of mountain shrublands using the sentinel-2 red-edge band. *Remote Sensing*, *11*(23). <https://doi.org/10.3390/rs11232807>
- Bréchnignac, F., Oughton, D., Mays, C., Barnthouse, L., Beasley, J. C., Bonisoli-Alquati, A., Bradshaw, C., Brown, J., Dray, S., Geras'kin, S., Glenn, T., Higley, K., Ishida, K., Kapustka, L., Kautsky, U., Kuhne, W., Lynch, M., Mappes, T., Mihok, S., ... Tsukada, H. (2016). Addressing ecological effects of radiation on populations and ecosystems to improve protection of the environment against radiation: Agreed statements from a Consensus Symposium.

- Journal of Environmental Radioactivity*, 158–159, 21–29. <https://doi.org/10.1016/j.jenvrad.2016.03.021>
- Carvalho, M., Cardoso-Fernandes, J., González, F. J., & Teodoro, A. C. (2025). Comparative Performance of Sentinel-2 and Landsat-9 Data for Raw Materials' Exploration Onshore and in Coastal Areas. *Remote Sensing*, 17(2). <https://doi.org/10.3390/rs17020305>
- Chen, Y., Wang, Y., Zhang, F., Dong, Y., Song, Z., & Liu, G. (2023). Remote Sensing for Lithology Mapping in Vegetation-Covered Regions: Methods, Challenges, and Opportunities. *Minerals*, 13(9), 1–26. <https://doi.org/10.3390/min13091153>
- Dong, T., Liu, J., Shang, J., Qian, B., Ma, B., Kovacs, J. M., Walters, D., Jiao, X., Geng, X., & Shi, Y. (2019). Assessment of red-edge vegetation indices for crop leaf area index estimation. *Remote Sensing of Environment*, 222 (December 2018), 133–143. <https://doi.org/10.1016/j.rse.2018.12.032>
- Hu, B., Xu, Y., Wan, B., Wu, X., & Yi, G. (2018). Hydrothermally altered mineral mapping using synthetic application of Sentinel-2A MSI, ASTER and Hyperion data in the Duolong area, Tibetan Plateau, China. *Ore Geology Reviews*, 101, 384–397. <https://doi.org/10.1016/j.oregeorev.2018.07.017>
- Koesuma, S., Putera, M. A. H., & Darsono. (2019). A Microtremor Analysis for Microzonation of Seismic Vulnerability Index by Using Horizontal to Vertical Spectral Ratio in The Southern Area of Klaten Regency. *Journal of Physics: Conference Series*, 1153(1), 1–6. <https://doi.org/10.1088/1742-6596/1153/1/012023>
- Laode, A. M. W., Massinai, M. A., Massinai, M. F. I., & Syamsuddin, E. (2025). Evaluating Liquefaction Susceptibility Through HVSR and MASW Methods: A Case Study in Mamuju, West Sulawesi, Indonesia. *Rudarsko-Geološko-Naftni Zbornik*, 40(5), 1–18. <https://doi.org/10.17794/rgn.2025.5.1>
- Liu, Y., Qian, J., & Yue, H. (2021). Comprehensive Evaluation of Sentinel-2 Red Edge and Shortwave-Infrared Bands to Estimate Soil Moisture. *IEEE Journal of Selected Topics in Applied Earth Observations and Remote Sensing*, 14, 7448–7465. <https://doi.org/10.1109/JSTARS.2021.3098513>
- Meilano, I., Salman, R., Susilo, S., Shiddiqi, H. A., Supendi, P., Lythgoe, K., Tay, C., Bradley, K., Rahmadani, S., Kristyawan, S., & Yun, S. H. (2023). The 2021 MW6.2 Mamuju, West Sulawesi, Indonesia earthquake: partial rupture of the Makassar Strait thrust. *Geophysical Journal International*, 233(3), 1694–1707. <https://doi.org/10.1093/gji/ggac512>
- Meraner, A., Ebel, P., Zhu, X. X., & Schmitt, M. (2020). Cloud removal in Sentinel-2 imagery using a deep residual neural network and SAR-optical data fusion. *ISPRS Journal of Photogrammetry and Remote Sensing*, 166(July), 333–346. <https://doi.org/10.1016/j.isprsjprs.2020.05.013>
- Nugraha, E. D., Hosoda, M., Kusdiana, Utara, Mellawati, J., Nurokhim, Tamakuma, Y., Ikram, A., Syaifudin, M., Yamada, R., Akata, N., Sasaki, M., Furukawa, M., Yoshinaga, S., Yamaguchi, M., Miura, T., Kashiwakura, I., & Tokonami, S. (2021). Comprehensive exposure assessments from the viewpoint of health in a unique high natural background radiation area, Mamuju, Indonesia. *Scientific Reports*, 11(1), 1–16. <https://doi.org/10.1038/s41598-021-93983-2>
- Nugraha, E. D., Hosoda, M., Tamakuma, Y., Kranrod, C., Mellawati, J., Akata, N., & Tokonami, S. (2021). A unique high natural background radiation area in Indonesia: a brief review from the viewpoint of dose assessments. *Journal of Radioanalytical and Nuclear Chemistry*, 330(3), 1437–1444. <https://doi.org/10.1007/s10967-021-07908-4>
- Perdana, M. J., & Amijaya, H. (2011). Source indication of oil seep from Paniki river, Kalukku, Mamuju, West Sulawesi based on geochemical characterization. *Proceedings JCM Makassar 2011*.
- Rahmaningrum, A. N. N. (2025). *Karakterisasi mineral Pembawa uranium pada Batuan vulkano-sedimenter kompleks Batuan gunung API adang di daerah botteng dan salumati, Sulawesi Barat*. ITB University.
- Rosianna, I., Nugraha, E. D., Syaeful, H., Putra, S., Hosoda, M., Akata, N., & Tokonami, S. (2020). Natural radioactivity of laterite and volcanic rock sample for radioactive mineral exploration in mamuju, indonesia. *Geosciences (Switzerland)*, 10(9), 1–13. <https://doi.org/10.3390/geosciences10090376>
- Rumora, L., Miler, M., & Medak, D. (2021). Contemporary comparative assessment of atmospheric correction influence on radiometric indices between Sentinel-2A and Landsat 8 imagery. *Geocarto International*, 36(1), 13–27. <https://doi.org/10.1080/10106049.2019.1590465>
- Saepuloh, A., Ratnanta, I. R., Hede, A. N. H., Susanto, V., & Sucipta, I. G. B. E. (2023). Radioactive remote signatures derived from Sentinel-2 images and field verification in West Sulawesi, Indonesia. *Environmental Monitoring and Assessment*, 195(10). <https://doi.org/10.1007/s10661-023-11868-5>
- Saputra, A., Abdullah, I., Dahnum, D., Mustika, D., Oktavianto, P., Noor, A. Z., Pamungkas, N. S., & Yusuf, M. (2025). Strategic utilization of covalent organic frameworks for uranium adsorption from high concentrate U–Th monazite sand: a review. *Journal of Radioanalytical and Nuclear Chemistry*, 334, 3843–3864. <https://doi.org/https://doi.org/10.1007/s10967-025-10135-w>
- Shaban, G., Fadlin, & Priadi, B. (2016). Geochemical signatures of potassic to sodic Adang Volcanics, Western Sulawesi: Implications for their tectonic setting and origin. *Indonesian Journal on Geoscience*, 3(3), 195–216. <https://doi.org/10.17014/ijog.3.3.195-214>
- Shebl, A., Badawi, M., Dawoud, M., Abd El-Wahed, M., El-Dokouny, H. A., & Csámer, Á. (2024). Novel comprehensions of lithological and structural features gleaned via Sentinel 2 texture analysis. *Ore Geology Reviews*, 168 (March 2023). <https://doi.org/10.1016/j.oregeorev.2024.106068>
- Sompotan, A. F. (2012). *Struktur Geologi Sulawesi*. Bandung Institute of Technology.
- Subasinghe, C. S., Ratnayake, A. S., Roser, B., Sudesh, M., Wijewardhana, D. U., Attanayake, N., & Pitawala, J. (2022). Global distribution, genesis, exploitation, applications, production, and demand of industrial heavy miner-

- als. *Arabian Journal of Geosciences*, 15(20). <https://doi.org/10.1007/s12517-022-10874-0>
- Sun, Y., Qin, Q., Ren, H., Zhang, T., & Chen, S. (2020). Red-Edge Band Vegetation Indices for Leaf Area Index Estimation from Sentinel-2/MSI Imagery. *IEEE Transactions on Geoscience and Remote Sensing*, 58(2), 826–840. <https://doi.org/10.1109/TGRS.2019.2940826>
- Supendi, P., Ramdhan, M., Priyobudi, Sianipar, D., Wibowo, A., Gunawan, M. T., Rohadi, S., Riama, N. F., Daryono, Prayitno, B. S., Murjaya, J., Karnawati, D., Meilano, I., Rawlinson, N., Widiyantoro, S., Nugraha, A. D., Marliyani, G. I., Palgunadi, K. H., & Elsera, E. M. (2021). Fore-shock–mainshock–aftershock sequence analysis of the 14 January 2021 (Mw 6.2) Mamuju–Majene (West Sulawesi, Indonesia) earthquake. *Earth, Planets and Space*, 73(1), 1–10. <https://doi.org/10.1186/s40623-021-01436-x>
- Vrdoljak, L., & Kilić Pamuković, J. (2022). Assessment of Atmospheric Correction Processors and Spectral Bands for Satellite-Derived Bathymetry Using Sentinel-2 Data in the Middle Adriatic. *Hydrology*, 9(12). <https://doi.org/10.3390/hydrology9120215>
- White, L. T., Hall, R., Armstrong, R. A., Barber, A. J., Boudagher, M., Baxter, A., Wakita, K., Manning, C., & Soesilo, J. (2017). Journal of Asian Earth Sciences The geological history of the Latimojong region of western Sulawesi, Indonesia. *Journal of Asian Earth Sciences*, 138, 72–91. <https://doi.org/10.1016/j.jseaes.2017.02.005>
- Wijaya, S. (2024). *Identifikasi radionuklida primordial pada tanah dan implikasinya terhadap lingkungan studi kasus : Desa Botteng, Kecamatan Simboro, Kabupaten Mamuju, Sulawesi Barat*. ITB University.
- Yu, D., & Fang, C. (2023). Urban Remote Sensing with Spatial Big Data: A Review and Renewed Perspective of Urban Studies in Recent Decades. *Remote Sensing*, 15(5), 1–34. <https://doi.org/10.3390/rs15051307>

SAŽETAK

Daljinsko istraživanje radioaktivnih alteracijskih zona korištenjem Sentinel-2 i SPAD mjerenja klorofila u Mamuju, Indonezija

Ova studija istražuje prirodnu radioaktivnu mineralizaciju (uranij-torij) u Mamuju, Zapadni Sulawesi, posebno unutar vulkana Adang kontroliranoga rasjedom, područja poznatoga po odstupanjima prirodnoga zračenja. Cilj je bio procijeniti stres vegetacije kao zamjenu za radioaktivnu mineralizaciju integrirajući satelitske podatke i terensku validaciju. Obradeni su podatci Sentinel-2A koristeći se omjerima pojasa ($4/2$ željezov oksid, $4/3$ ferično željezo, $11/12$ glina) i kompozitima lažnih boja kako bi se odredile zone promjena. Indeks vegetacije crvenoga ruba (REVI; B₃, B₄, B₆) izračunan je za otkrivanje stresa vegetacije. Terenskim radom u prosincu 2023. prikupljeno je 68 SPAD mjerenja klorofila iz paprati, interpoliranih s inverznim ponderiranjem udaljenosti i uspoređenih s neovisnim brzinama doze zračenja. Rezultati pokazuju snažnu korelaciju između REVI-ja i SPAD-a ($R^2 = 0,76$), što potvrđuje osjetljivost pojasa crvenoga ruba na varijabilnost klorofila. Vrijednosti SPAD-a znatno su se smanjile u zonama visokoga zračenja pokazujući snažnu negativnu korelaciju s brzinom doze ($R^2 = 0,90$). Vrijednosti od 4 do 40 bile su tipične u područjima s odstupanjima zračenja, dok su vrijednosti >40 karakterizirale nižu izloženost. Anomalije vegetacijskoga stresa i indeks klorofila dobiven satelitskim putem prostorno su se preklapali sa zonama alteracija i bili su koncentrirani u vulkanima Adang duž strukturnih kontrola. Razlike u vrstama paprati upućuju na različitu osjetljivost na zračenje. Ovaj integrirani pristup pokazuje učinkovitost kompozita alteracija Sentinel-2, REVI-ja i SPAD validacije kao brzoga i jeftinoga okvira za rano istraživanje radioaktivnih minerala, a istovremeno doprinosi procjeni opasnosti od zračenja okoliša.

Ključne riječi:

Sentinel-2, indeks vegetacije crvenoga ruba (REVI), SPAD klorofil, radioaktivna mineralizacija, Mamuju

Author's contribution

Nuraisyah Pertiwi Kamsir (M.T.): conceptualization, data curation, investigation, formal analysis, visualization, and writing – original draft. **Asep Saepuloh** (Dr. Eng.): supervision, methodology, validation, resources, and writing – review & editing. **Very Susanto** (Dr. Eng.): software, data curation, formal analysis, visualization, and writing – review & editing. **Eka Djatnika Nugraha** (Dr.): investigation, validation, resources, and writing – review & editing. All authors have read and agreed to the published version of the manuscript.